Petroleum Science 18 (2021) 1219–1229

Contents lists available at ScienceDirect

Petroleum Science

journal homepage: www.keaipublishing.com/en/journals/petroleum-science

Original Paper

Corrosion risk analysis of tube-and-shell heat exchangers and design of outlet temperature control system

Hao-Zhe Jin [a, *], Yong Gu [a], Guo-Fu Ou [b]

[a] The Institute of Flow-Induced Corrosion, Zhejiang Sci-tech University, Hangzhou, 310000, Zhejiang, China
[b] Institute of Flow Induced Corrosion and Intelligent Prevention and Control, Changzhou University, Changzhou, 213000, Jiangsu, China

ARTICLE INFO

Article history:
Received 4 May 2020
Accepted 16 November 2020
Available online 8 July 2021

Edited by: Xiu-Qiu Peng

Keywords:
Shell-and-tube heat exchanger
Corrosion risk
Dynamic model
Fuzzy logic control
PID control

ABSTRACT

This study deals with the high-risk shell-and-tube heat exchangers in the effluent system of hydrogenation reaction of the petrochemical industry. The process of hydroprocessing reactor effluent system is simulated in Aspen Plus to study the distribution of corrosive medium in the three phases of oil, gas and water. The least-squares method is utilized to calculate the ammonium salt crystallization temperature. Then, the heat exchanger with risk of ammonium salt crystal corrosion is identified. Dynamic mathematical modeling of the heat exchanger is established to determine the transfer function. A temperature control system with proportional integral derivative (PID) control of the heat exchanger outlet is designed, and fuzzy logic is used to implement self-tuning of PID parameters. After MATLAB simulation, the results show the control system can achieve rapid control of the heat exchanger outlet temperature.

1. Introduction

Heat exchangers are ubiquitous pieces of equipment in the process industry, especially in the petrochemical industry (Panahi et al., 2020). The more common type of heat exchangers is represented by the shell-and-tube heat exchanger (Fettaka et al., 2013), which has the advantages of simple structure, wide selection of materials, low cost and large processing capacity. In the refinery unit, heat exchangers have been subjected to high-temperature and high-pressure conditions for a long time, and are in a complex corrosion environment of flow, mass transfer, cooling, and phase change (Rizk et al., 2017; Rezaei et al., 2021; Faes et al., 2019). It is internationally recognized as the high-risk equipment for corrosion. The proportion of processing of inferior crude oils of high sulfur, high acid, and containing chlorine has been increasing in recent years, thereby resulting in failure incidents in the heat exchangers of crude unit and hydrogenation unit (Jin et al., 2017; Zhang et al., 2013; Xu et al., 2013). Due to corrosion, the heat transfer efficiency of the heat exchanger is reduced, resulting in an increase in the outlet temperature, which also affects the subsequent process flow and even reduces the final product's quality. At the same time, more than 80% of worldwide energy utilization involve heat transfer processes (Chen et al., 2009; Laszczyk, 2017). Therefore, designing a suitable control system can not only control the temperature of the heat exchanger outlet, but also improve the heat transfer efficiency and economic efficiency (Bauer et al., 2008; Rhinehart et al., 2017; Dulău et al., 2018; Ramadan et al., 2016).

Process simulation combined with Computational Fluid Dynamics (CFD) numerical calculation is an effective method to analyze the ammonium salt deposition (Ou et al., 2013; Jin et al., 2019). Ionic equilibrium model can be created by Aspen software to calculate the crystal temperature of the NH_4Cl. And it will determine whether the equipment in the corrosion circuit is at risk of corrosion, especially heat exchangers. In view of the rise in outlet temperature caused by corrosion of the heat exchanger, an appropriate control method should be adopted to improve the heat exchange efficiency. Control of heat exchangers is a complex process due to the nonlinear behavior and complexity caused by various phenomena such as leakage, friction, temperature dependent flow properties, unknown fluid properties. Various control strategies were designed for overcoming mentioned problems. A control strategy is proposed by Gang et al. (2013) for cooling season as to compare the temperatures of the water exiting the ground heat exchanger and the cooling tower directly. They develops artificial neural network models for predicting the temperature and the results show that the model can predict temperature with an

* Corresponding author.
E-mail address: haozhejin@zstu.edu.cn (H.-Z. Jin).

https://doi.org/10.1016/j.petsci.2021.07.002

List of symbols

Kp	The ammonium salt dissociation constant, Pa^2
T	Temperature, K
TJ	The crystallization temperature of NH_4Cl, K
G_1	The flow rates of hot fluids, kg/s
G_2	The flow rates of cold fluids, kg/s
T_{1i}	The inlet temperatures of hot fluids, K
T_{2i}	The inlet temperatures of cold fluids, K
T_{1o}	The outlet temperature of the hot fluids, K
T_{2o}	The outlet temperature of the cold fluids, K
c_1	The specific heat capacities of the hot fluid, J/(kg·K)
c_2	The specific heat capacities of the cold fluid, J/(kg·K)
q	Heat transfer rate, J
k	Heat transfer coefficient, $W/m^2 \cdot K$
F	Heat transfer area, m^2
C	The circumference of the tube, m
L	The total length of the heat exchanger, m
M_1	The mass per unit length of the fluid, kg
W	The capacity of the heat exchanger, m^3
W_1	The storage capacity of hot fluid, m^3
W_2	The storage capacity of cold fluid, m^3
s	Laplacian
K_p	Proportional coefficient
K_i	Integration constant
K_d	Differential constant
E	The inlet flow deviation
Ec	The deviation change rate
tp	Peak time, s
ts	Adjustment time, s
ess	The steady-state error

Greek letters

μ	The peak position of the Gaussian curve
σ	Overshoot
δ	Standard deviation of the Gaussian curve
ε_i	The measurement error

absolute error less than 0.2 K. Wang et al. (2013) presents an adaptive optimal control strategy for online control of complex chilled water systems involving intermediate heat exchangers. Adaptive method is utilized to update the key parameters of the proposed models online. The results demonstrate that the strategy has enhanced control robustness and reliability. Gao et al. (2015) solved an established thermal dynamic model numerically to predict the transient response of an unmixed–unmixed cross-flow heat exchanger and analyzed the transient response due to the time dependent fluid inlet temperature and flow rate are conducted. Vasickaninova et al. (2018) applied a variety of robust control techniques to laboratory heat exchangers with nonlinear and asymmetric properties that can be modeled as uncertain systems. Considering incomplete knowledge margin of process parameters, parameter changes and measurement noise, real-time control of the heat exchanger under laboratory conditions is achieved. The control effects of different robust controllers are compared through three indicators, which show that the robust controllers have good control performance. Skavdahl et al. (2016) take the advanced high temperature reactor-intermediate heat exchanger-secondary heat exchanger (SHX) system as the research object. Transfer functions describing relationships between the controlled variables and the manipulated and load variables are developed and the system response to various temperature disturbances is simulated using a custom-developed MATLAB program. Simulation results indicate that the controlled variables are maintained successfully at their desired points by the control system. Since the characteristics of the industrial heat exchange system (HES) are drastically affected by variations of the steam pressure, ambient temperature and water quality, some control strategy are established, such as the cascade PI control strategy with the signal compensation (Jia et al., 2020), a dual-rate adaptive control method (Wang et al., 2018), the neural network MPC method (Carvalho et al., 2020) and so on.

However, a major problem of the above mentioned methods are that it is relatively difficult to construct an accurate mathematical model of the heat exchanger. This paper analyzes the process of the hydroprocessing reactor effluent system. The crystallization temperature of ammonium chloride salt is obtained by combining Aspen Plus software and least square method, and the heat exchanger with corrosion risk is determined. The mathematical model of the heat exchanger is established, and a fuzzy PID control system is designed to control the outlet temperature of the heat exchanger. On the one hand, the research of this paper provides a characterization method for the risk analysis of the hydroprocessing reactor effluent system. On the other hand, the fuzzy PID control system designed in this paper can provide guidance to the outlet temperature control of the heat exchanger.

2. Corrosion risk assessment

2.1. Technological process

Hydroprocessing reactor effluent separation and cooling system is illustrated in Fig. 1. The hydroprocessing effluent flows out from the bottom of the hydroprocessing reactor (R301) at a temperature of 611.75 K. It is cooled to 464.05 K by two heat exchangers (E301 and E302) and then enters the heat exchanger (E303). The outlet temperature of the heat exchanger (E303) is 388.55 K. After cooling by air cooler (A301) and water cooler (E304), it enters the high-pressure separator (D301). The recycle hydrogen flows out of the top of D301 to the desulfurization tower, the sour water flows out from the bottom of D301, and the oil phase enters the low-pressure separator (D302), where the sour gas, cold effluent liquid and sour water are separated. The cold effluent liquid is transported to the fractionation system. The inlet of the heat exchanger (E303) is provided with intermittent water injection point, which temperature is 320.15 K. The source of water injection is the demineralized water and the purified water after demineralization. During the cooling process of NH_3, HCl and H_2S generated by hydrogenation reaction into heat exchanger (E301, E302, E303), air cooler (A301) and water cooler (E304), with the decrease of process logistics temperature, crystallization reaction of NH_3 in gas phase will occur with HCl and H_2S to produce NH_4Cl and NH_4HS crystal particles. Ammonium salt particles are easy to absorb water in the fluid or dissolve in the water phase to form a high concentration of corrosive solution, resulting in the occurrence of ammonium salt crystal deposition and corrosion under scale, resulting in equipment corrosion failure. Therefore, it is of great significance to take the temperature of the ammonium salt crystallization as an index to evaluate the corrosion risk of the hydrogenation effluent system. By calculating the ammonium salt crystallization temperature, the position in the process that corresponds to the temperature will be determined, so as to identify which equipment or section of

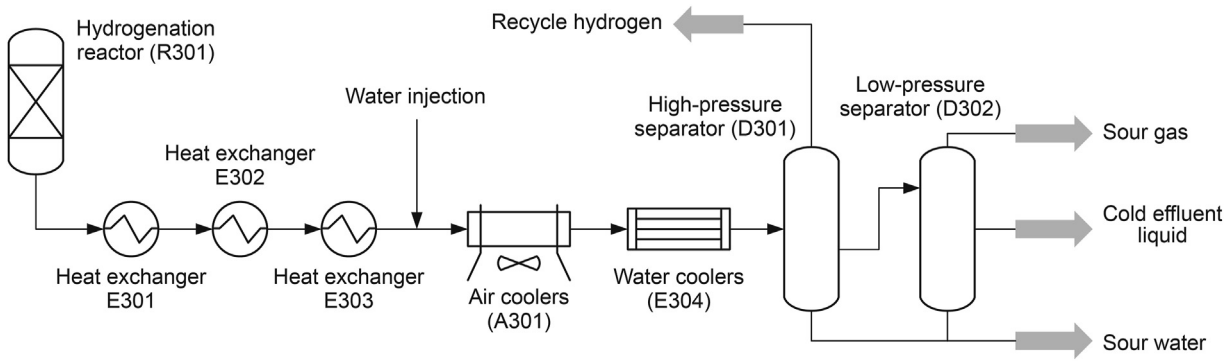

Fig. 1. Hydroprocessing reactor effluent separation and cooling system.

pipeline risk of ammonium salt crystallization corrosion exists.

2.2. Crystal temperature calculation method

Depending on the principle of material conservation, combining the analysis data and real-time monitoring data obtained from the Laboratory Information Management System (LIMS) and the Distributed Control System (DCS), the composition of the hydroprocessing reactor effluent can be reversed. In Aspen Plus, the heat exchanger module and flash module were applied in the preparation of the multiphase equilibrium system of hydrogenation effluent system. The temperature, pressure and flow of heat transfer and flash evaporation system adopt the real-time data collected by DCS, and the equilibrium distribution law of NH_3, HCl and H_2S in three phases can be obtained by changing the contents of S, N and Cl. The simulation model is presented in Fig. 2 and solved by the Peng-Robinson method.

In Fig. 2, the meaning of letters is shown in Table 1 below. The numbers 1–7 represent simulation modules, where 1 and 5 are mixer model, 2, 3, 4 and 6 are heater model, 7 is a separator.

In the actual working condition, the crude oil feed quantity is 22.38 kg/s, the chlorine content is 1 ppm, the nitrogen content is 678.225 ppm, the sulfur content is 0.53%, the water content is 1.94 kg/s and the pressure is 6.9×10^6 Pa. According to the simulation results, the curve of partial pressure product *Kp* of and HCl, H_2S and NH_3 changing with temperature in the gas phase at three-phase equilibrium is drawn in MATLAB, and the intersection point of the curve of crystallization equilibrium when the crystallization reaction of NH_4Cl and NH_4HS reached equilibrium obtained by thermodynamic calculation is the crystallization temperature of NH_4Cl and NH_4HS, as shown in Fig. 3 and Fig. 4.

In Fig. 4, the crystallization line of NH_4HS is above the curve of value of *Kp* in actual conditions. There is no intersection of two lines, which illustrate that NH_4HS crystallization is not produced in the hydrogenation effluent system.

In Fig. 3, the upper part of the NH_4Cl crystal equilibrium curve indicates that NH_4Cl is solid, that is, there is a risk of crystallization. The lower part indicates that NH_3 and HCl exist in the form of gas, and crystallization will not occur at the corresponding temperature. The intersection of the two curves in the figure is the temperature point at which NH_4Cl begins to crystallize. In the actual working condition, NH_4Cl crystallization will occur when the

Table 1
The meaning of letters.

Letters	Material
S1	Recycle hydrogen
S2	Low-pressure segregator oil
S3	S, Cl, N content in raw materials
S4	Low-pressure segregator gas
S5–S10	Hydroprocessing reactor effluent at different temperatures
S11	Gas phase after separation
S12	Oil phase after separation
S13	Water phase after separation
S14	Water injection

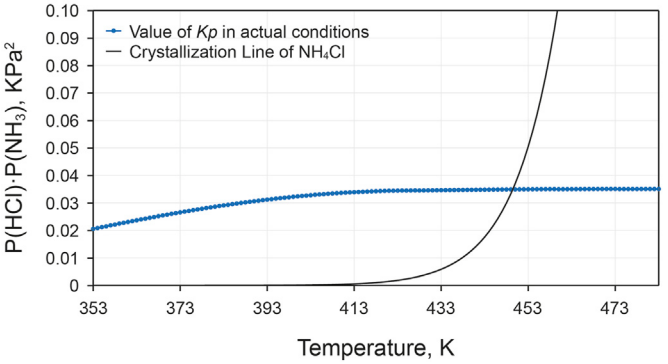

Fig. 3. The calculation of the crystallization temperature of NH_4Cl.

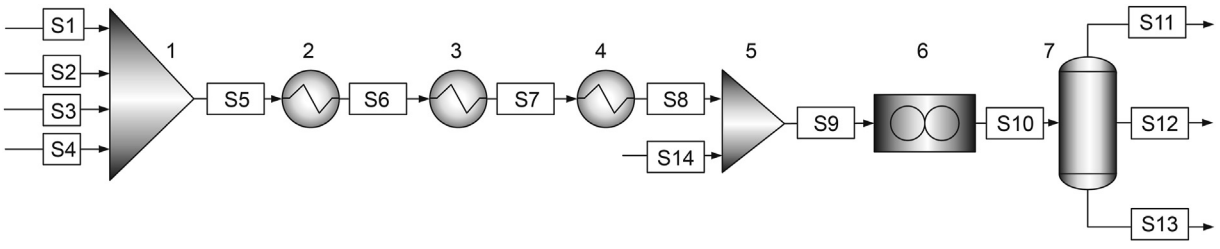

Fig. 2. The simulation model in Aspen Plus.

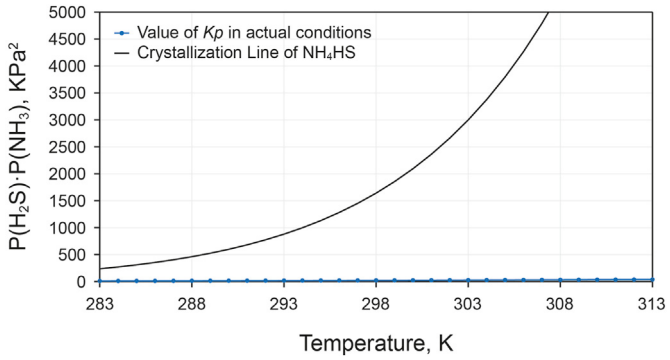

Fig. 4. The calculation of the crystallization temperature of NH_4HS.

hydroprocessing reactor effluent are cooled to the crystallization point during the cooling process. There is risk of NH_4Cl crystallization corrosion in the equipment below this temperature, and prevention and control measures should be taken. In order to accurately calculate the crystallization temperature, gaussian fitting is carried out on the two curves in this paper and specific steps are as follows.

1) Assume a set of experimental data by (x_i, y_i) $(i = 1, 2, 3, \ldots, N)$, which can be described by a Gaussian function.

$$y_i = A \times e^{-\frac{(x_i-\mu)^2}{2\delta^2}} \tag{1}$$

The parameter to be estimated in Eq. (1) is A. The physical meanings represented by μ and σ are the peak position, and standard deviation of the Gaussian curve.

2) Take the natural logarithm of both sides of Eq. (1)

$$\ln y_i = \ln A - \frac{(x_i-\mu)^2}{2\delta^2} = (\ln A - \frac{\mu^2}{2\delta^2}) + \frac{2x_i\mu}{2\delta^2} - \frac{x_i^2}{2\delta^2} \tag{2}$$

3) Parameter substitution for Eq. (2)

$$\ln y_i = z_i \tag{3}$$

$$\ln A - \frac{\mu^2}{2\delta^2} = b_0 \tag{4}$$

$$\frac{2\mu}{2\delta^2} = b_1 \tag{5}$$

$$-\frac{1}{2\delta^2} = b_2 \tag{6}$$

Then Eq. (2) becomes a quadratic polynomial fitting function.

$$z_i = b_0 + b_1x_i + b_2x_i^2 = (1\ x_i\ x_i^2)\begin{bmatrix} b_0 \\ b_1 \\ b_2 \end{bmatrix} \tag{7}$$

Consider the measurement error ε_i, which caused by the calculation of data y_i during the experiment. Then, express z_i in matrix form as follows:

$$\begin{bmatrix} z_1 \\ z_2 \\ \vdots \\ z_n \end{bmatrix} = \begin{bmatrix} 1 & x_1 & x_1^2 \\ 1 & x_2 & x_2^2 \\ \vdots & \vdots & \vdots \\ 1 & x_n & x_n^2 \end{bmatrix} \begin{bmatrix} b_0 \\ b_1 \\ b_2 \end{bmatrix} + \begin{bmatrix} \varepsilon_1 \\ \varepsilon_2 \\ \vdots \\ \varepsilon_n \end{bmatrix} \tag{8}$$

Abbreviated as

$$\boldsymbol{Z}_{n\times1} = \boldsymbol{X}_{n\times3}\boldsymbol{B}_{3\times1} + \boldsymbol{E}_{n\times1} \tag{9}$$

(4) Without considering the influence of the total measurement error $\boldsymbol{E}_{n\times1}$, according to the principle of least squares, the fitting constants b_0, b_1, b_2 can be obtained. The generalized least squares solution of the matrix $\boldsymbol{B}$ is:

$$\boldsymbol{B} = \left(\boldsymbol{X}^{\mathrm{T}}\boldsymbol{X}\right)^{-1}\boldsymbol{X}^{\mathrm{T}}\boldsymbol{Z} \tag{10}$$

After solving for $\boldsymbol{B}$, bring b_0, b_1, b_2 into Eq. (4), Eq. (5), Eq. (6), find the values of A, μ and δ. Then get the fitting function. Assume that the fitted functions are respectively as follows:

$$h_1 = f_1(x) \tag{11}$$

$$h_2 = f_2(x) \tag{12}$$

Solve the intersection of the two curves using the secant method. Let the objective function be $H(x)$, x_k, x_{k-1} is the approximate root of $H(x) = 0$, then $H(x)$ is

$$H(x) = h_1 - h_2 = f_1(\mathrm{x}) - f_2(x) \tag{13}$$

Use $H(x_k)$, $H(x_{k-1})$ to construct a linear interpolation polynomial $P_1(x)$, and use the root of $P_1(x)$ as the new approximate root x_{k+1} of $H(x) = 0$

$$P_1(x) = H(x_k) + \frac{H(x_k) - H(x_{k-1})}{x_k - x_{k-1}}(x - x_k) \tag{14}$$

The iterative formula is solved as

$$x_{k+1} = x_k - \frac{H(x_k)}{H(x_k) - H(x_{k-1})}(x_k - x_{k-1}) \tag{15}$$

Determine whether it is less than the given error, which is the error between two adjacent iteration points artificially set. If the condition is met, the iteration ends, and x_{k+1} is the solution of $H(x) = 0$. Otherwise, continue the iteration until the result meets the end condition.

Aspen Plus simulation is performed on the working conditions of the device, and the obtained temperatures T and Kp are used as a

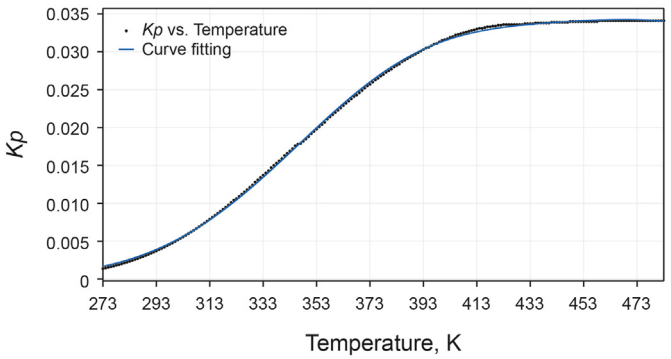

Fig. 5. The Gaussian fitting results of actual working conditions.

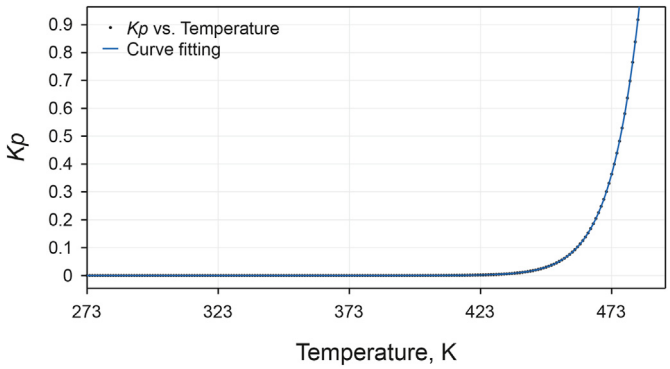

Fig. 6. The fitting result of the crystallization equilibrium curve.

set of experimental data. Gaussian fitting results are shown in the Fig. 5.

The fitted equations is:

$$Kp = 0.03215 \times e^{-\frac{(T_i-505.45)^2}{104.2^2}} + 0.02065 \times e^{-\frac{(T_i-388.15)^2}{71.16^2}} \quad (16)$$

The fitting error is expressed by root mean square error (RMSE), which is equal to 1.6538×10^{-4}.

In the same way, the fitting result of the crystallization equilibrium curve when the NH_4Cl crystallization reaction reaches equilibrium by thermodynamic calculation is shown in Fig. 6.

The fitted equations is:

$$Kp = 18780 \times e^{-\frac{(T_i-702.55)^2}{69.63^2}} \quad (17)$$

And RMSE is 5.0301×10^{-5}.

In order to solve the intersection point of the two curves, that is, the crystallization temperature of the ammonium chloride salt, the variance is obtained by the string cut method as follows:

$$H(T_i) = 18780 \times e^{-\frac{(T_i-702.55)^2}{69.63^2}} - 0.03215 \times e^{-\frac{(T_i-505.45)^2}{104.2^2}} - 0.02065 \times e^{-\frac{(T_i-388.15)^2}{71.16^2}} \quad (18)$$

During the iteration process, the relationship between the number of iteration steps and T_i is shown in the Fig. 7.

It can be seen from the Fig. 7 that when the string cut method is iterated to the fourth step, the given error requirements have been met, that is, the zero point of the function is $TJ = 449.3377$ K, which is the crystallization temperature of NH_4Cl under this working condition. It can be seen from the process flow that the inlet and outlet temperatures of the heat exchanger E303 are 464.05 K and 388.55 K, respectively, and the crystallization temperature of NH_4Cl is within this temperature range, indicating that there is a risk of NH_4Cl crystallization corrosion in the heat exchanger. NH_4Cl crystals deposited in the heat exchanger are removed, and the water injection point is selected to be the pipeline between E303 and E202.

2.3. Corrosion risk analysis

The content of Cl and N in crude oil is not fixed, sometimes it fluctuates greatly, and the change of pressure will also affect the partial pressure of NH_3 and HCl. Therefore, it is necessary to calculate and analyze the crystallization temperature of ammonium salt with changed conditions of Cl, N content and pressure, so as to judge the corrosion risk.

The content of Cl element in the effluent of hydrogenation reaction is generally 0.5–10 ppm, and the content of N is generally between 500 and 5000 ppm. According to the operating conditions, the system is divided into high pressure and low pressure, which will affect the operation of the system. The working conditions of each group of experiments are given in Table 2. The calculation results are presented in Fig. 8, Fig. 9 and Fig. 10.

Fig. 8 shows the change of crystallization temperature of NH_4Cl under different system operating pressure. With the increase of system pressure, the crystallization temperature of NH_4Cl increases gradually. As can be observed in Figs. 9 and 10, with the increase of Cl content and N content, the crystallization temperature of NH_4Cl increases significantly, and the crystallization risk of ammonium salt in the hydroprocessing reactor effluent system also increases continuously. It can be seen that the Cl content and N content in crude oil have a significant influence on the crystallization temperature of NH_4Cl, and it is very necessary to control the Cl content and N content in crude oil to reduce the crystallization temperature of NH_4Cl and avoid NH_4Cl crystallization deposition, tube blockage

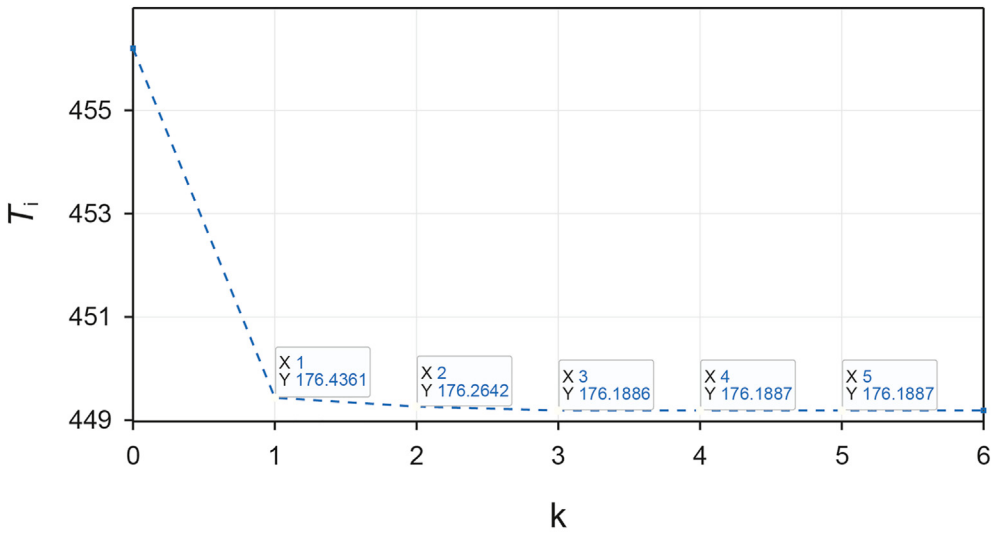

Fig. 7. The relationship between the number of iteration steps and T_i.

Table 2
Working conditions of each experiment.

Experiment	Content				
	S content, %	N content, ppm	Cl content, ppm	Water injection, kg/s	Pressure, Pa
①	0.53	678.225	1	1.94	$(1-13) \times 10^6$
②	0.53	678.225	0.5–10	1.94	6.9×10^6
③	0.53	500–5000	1	1.94	6.9×10^6

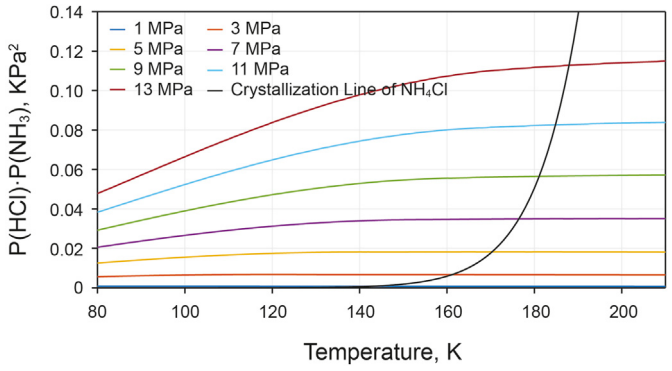

Fig. 8. Experiment ① the influence of operating pressure on the crystallization temperature of NH_4Cl.

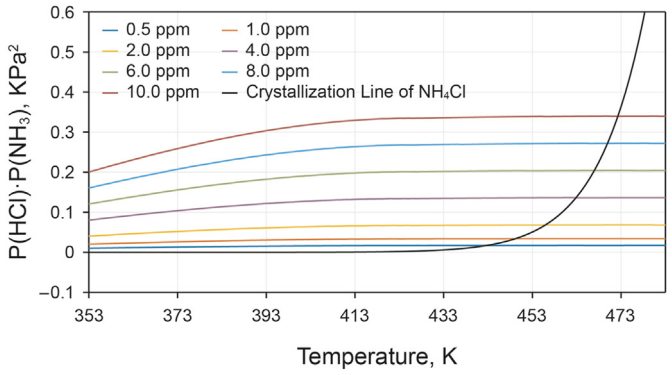

Fig. 9. Experiment ② the influence of Cl content on the crystallization temperature of NH_4Cl.

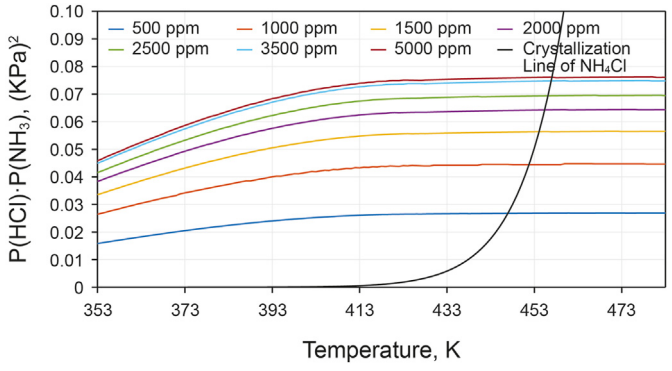

Fig. 10. Experiment ③ the influence of N content on the crystallization temperature of NH_4Cl.

at high temperature.

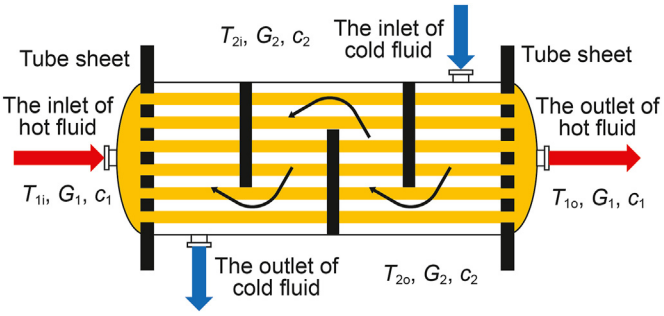

Fig. 11. Shell-and-tube heat exchanger.

3. Mathematical model

The structure of the shell-and-tube heat exchanger is shown in Fig. 11, where G_1 and G_2 are the flow rates of hot and cold fluids respectively and the unit is kg/h. T_{1i} and T_{2i} are the inlet temperatures of hot and cold fluids, and the unit is K. T_{1o} and T_{2o} are the outlet temperature of the hot and cold fluids, and the unit is K. c_1 and c_2 are the specific heat capacities of the hot fluid and the cold fluid, and the unit is J/(kg·K).

3.1. Static characteristics analysis

Static characteristic is that the output variable of the object under stable conditions is usually a functional relationship between the controlled variable and the input variable. The heat exchanger can be expressed in functional form as follows:

$$T_{1o} = f(T_{1i}, T_{2i}, G_1, G_2) \tag{19}$$

The two basic equations derived from the static characteristics—the heat balance relationship and the heat transfer rate equation are shown in Eq. (20) and Eq. (21) respectively.

$$q = G_1 c_1 (T_{1o} - T_{1i}) = G_2 c_2 (T_{2i} - T_{2o}) \tag{20}$$

$$q = kF\Delta T \tag{21}$$

Where q is heat transfer rate, J. k is heat transfer coefficient, W/m^2·K. F is heat transfer area, m^2. ΔT is the average temperature difference, K. The calculation formula of ΔT is as follows:

$$\Delta T = \frac{(T_{2i} - T_{1o}) + (T_{2o} - T_{1i})}{2} \tag{22}$$

Then put Eq. (20) and Eq. (22) into Eq. (21). Basic expressions of static characteristics of heat exchangers is as follows.

$$\frac{T_{1o} - T_{1i}}{T_{2i} - T_{2o}} = \frac{1}{\frac{G_1 c_1}{kF} + \frac{1}{2}\left(1 + \frac{G_1 c_1}{G_2 c_2}\right)} \tag{23}$$

Derivation of Eq. (23) can get the influence of G_1 on T_1 as follows.

$$\frac{dT_{1o}}{dG_1}=\frac{G_2c_2(T_{2i}-T_{1i})}{2{G_1}^2c_1[\frac{G_2c_2}{kF}+\frac{1}{2}(1+\frac{G_2c_2}{G_1c_1})]^2} \tag{24}$$

3.2. Dynamic characteristics analysis

Supposing that there is no phase change occurs on both sides of the heat exchanger. The dynamic characteristics of the heat exchanger is necessary to be described by partial differential equations. A mathematical model of the distributed parameter object is created. Start with the heat dynamic equilibrium equation, take a micro-element to analyze the problem, and assume that the temperature at each point in the micro-element is the same. Firstly, analyze the heat balance problem of hot fluid. Taking a cylinder of length dz as a micro-element. The thermal equilibrium equation of this micro-element can be described as:

$$G_1c_1T_1(l,t)-G_1c_1[T_1(l,t)+\frac{\partial T_1(l,t)}{\partial l}dl]+KCdl[T_2(l,t)-T_1(l,t)] = M_1c_1dl\frac{\partial T_1(l,t)}{\partial l} \tag{25}$$

Where, $l=z/L$. L is the total length of the heat exchanger, m. C is the circumference of the tube, m. Cdl is the surface area of the micro element, m^2. M_1 is the mass per unit length of the fluid, kg. M_1dl is the mass of the micro element, kg. Eliminate the dl in Eq. (25), and arrange it as

$$(\frac{M_1}{G_1})\frac{\partial T_1(l,t)}{\partial t}=-\frac{\partial T_1(l,t)}{\partial l}+(\frac{KC}{G_1c_1})[T_2(l,t)-T_1(l,t)] \tag{26}$$

Similarly, the heat balance equation of cold fluid is:

$$(\frac{M_2}{G_2})\frac{\partial T_2(l,t)}{\partial t}=-\frac{\partial T_2(l,t)}{\partial l}+(\frac{KC}{G_2c_2})[T_1(l,t)-T_2(l,t)] \tag{27}$$

The boundary conditions are:

$$T_1(l,0)=T_1(l) \tag{28}$$

$$T_2(l,0)=T_2(l) \tag{29}$$

$$T_1(0,t)=T_{1i}(t) \tag{30}$$

$$T_1(l,t)=T_{1o}(t) \tag{31}$$

$$T_2(0,t)=T_{2o}(t) \tag{32}$$

$$T_2(l,t)=T_{1i}(t) \tag{33}$$

It is difficult to solve dynamic equations accurately. In order to explain the basic laws of the dynamic characteristics of heat transfer objects, some empirical formulas can also be employed to describe them. The dynamic characteristics of the heat exchanger can be reflected in the following approximate relationship.

(1) The effect of T_{2i} on T_{1o} is described by the transfer function as follows:

$$G(s)=\frac{K}{Ts+1} \tag{34}$$

Where K is gain, s is Laplace operator, and $T=W/G_2$. W is the capacity of the heat exchanger, m^3.

(2) The effect of G_1 and G_2 on T_{1o} are described by the transfer function as follows:

$$G(s)=\frac{K}{(T_1s+1)(T_2s+1)}e^{-T_2s} \tag{35}$$

Where the calculation of T_1 and T_2 are as follows:

$$T_1=\frac{W_1/G_1+W_2/G_2}{2} \tag{36}$$

$$T_2=\frac{W_1/G_1+W_2/G_2}{8} \tag{37}$$

Where W_1 and W_2 are the storage capacity of hot and cold fluid respectively, m^3.

From the transfer function, it can be approximated that the dynamic characteristic has a purely delayed second-order inertial link. To transfer heat from the hot fluid to the cold, the hot fluid must first be transferred to the partition wall, and then from the partition wall to the cold fluid. This grows up to be a second-order inertial link. In addition, pure hysteresis due to residence time is also considered. The two time constants T_1 and T_2 of the second-order link depend not only on the residence time of the fluid on both sides, but also on the thickness, material and scaling of the tube. However, Eq. (35) describes the inherent nature of the dynamic characteristics of the heat exchanger.

(3) In the heat exchanger outlet temperature control system, the hot fluid flow G_1 does not change. According to the working condition, the basic law of the dynamic characteristics of the heat exchanger can be achieved. The mathematical model of heat exchanger temperature control is

$$G(s)=\frac{2}{537s^2+57.17s+1}e^{-11.85s} \tag{38}$$

It can be seen from the above equation that the system lag time constant is 11.85s. And the heat exchanger temperature control system is a system with a large inertia and lag.

4. Design and simulation of fuzzy logic control system

4.1. Fuzzy logic control

The heat exchanger outlet temperature control system is a typical non-linear control system. Non-linear controller design is an important task for the petrochemical industry (Aras et al., 2011; Lin et al., 2020). Non-linear controllers have the ability to deal with common process characteristics, such as input and measured dead time, uncertain and changing parameters, manipulation and state variable constraints, unmeasured and frequent disturbances, etc (Fuente et al., 2006; Wakitani et al., 2019). Fuzzy control is an intelligent control method based on fuzzy set theory, fuzzy linguistic variables and an inference engine. It is an intelligent control method that imitates human fuzzy inference and decision-making processes of human behavior. The structure principle of fuzzy controller is illustrated in Fig. 12.

It is useful for representing process descriptions such as high or low, which are inherently fuzzy and involve qualitative conceptualizations of numerical values meaningful to operators (Geng et al., 2009; Hojjati et al., 2007). Fuzzy logic supports representation of variables and relationships in linguistic terms. For example, the linguistic variable of pipe temperature can take the fuzzy values of low, normal, high, and very high, and each fuzzy value can be modeled.

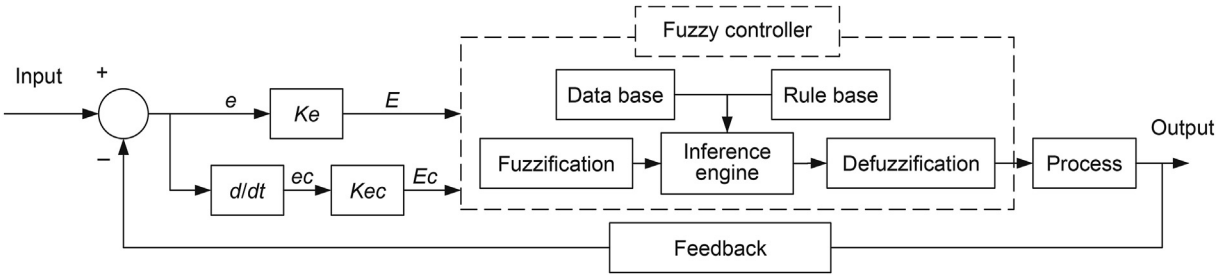

Fig. 12. The structure principle of Fuzzy logic controller.

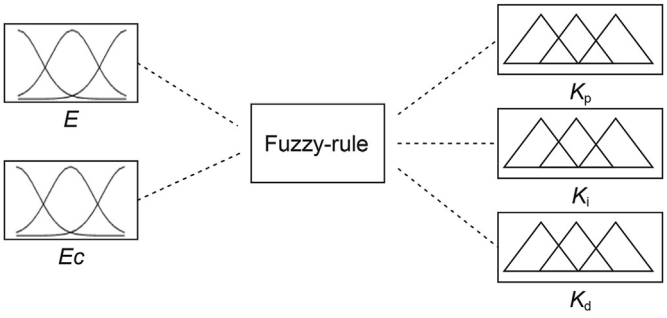

Fig. 13. The relationship between the input and output variables.

4.2. Fuzzy-PID control

This paper adopts the method of combining fuzzy control technology with PID control. $E(k)$ and $Ec(k)$ are input deviation and deviation change rate of the system, respectively. K_p, K_i, K_d are the parameters that characterize their proportional (P), integral (I) and differential (D) effects. However, the PID regulator does not possess the function of setting parameters online, so it can not satisfy the self-tuning requirements of the system under different working conditions, thereby affecting the further improvement of its control effect.

Fuzzy-PID uses fuzzy set theory to establish a binary continuous function relationship between the parameters K_p, K_i, K_d and the input deviation E and deviation change rate Ec.

Depending on the control object of the system is the heat exchanger inlet flow rate, the two-input three-output controller can comply with the requirements. The values of the inlet flow deviation E and the deviation change rate Ec of the heat exchanger are input variables, and K_p, K_i, K_d are output variables. If NB, NM, NS, ZO, PS, PM, PB are used to denote negative large, negative medium, negative small, zero, positive small, positive medium, positive large, etc., in this system, E, Ec and output K_p, K_i, K_d is specified as the following fuzzy subsets:

E, Ec = {NB, NM, NS, ZO, PS, PM, PB}

K_p, K_i, K_d = {NB, NM, NS, ZO, PS, PM, PB}

Their domains are:

E, Ec = {-3, −2, −1, 0, 1, 2, 3}

K_p, K_i, K_d = {0, 1, 2, 3, 4, 5, 6}

The relationship between the input and output variables and the

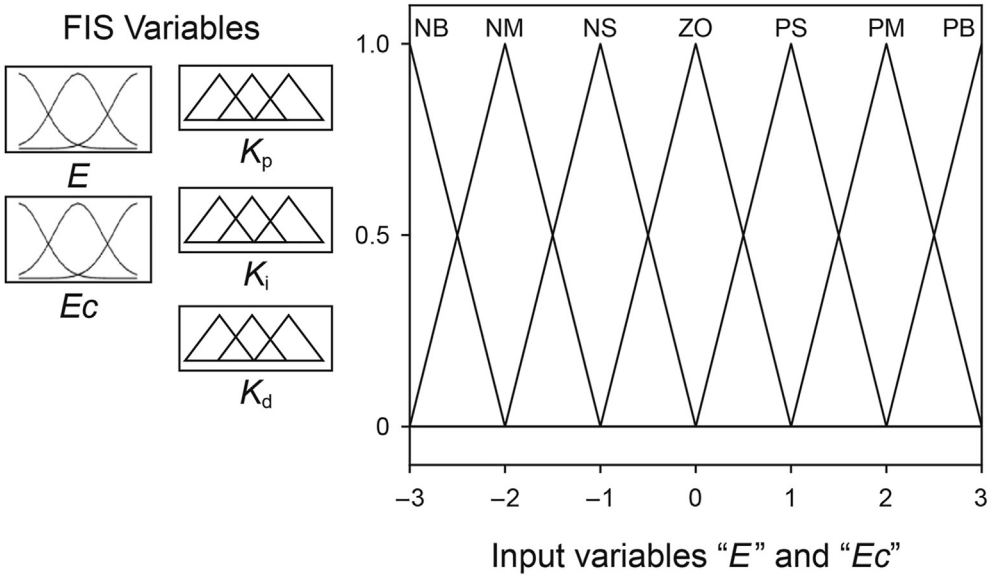

Fig. 14. The membership function of E and E_c.

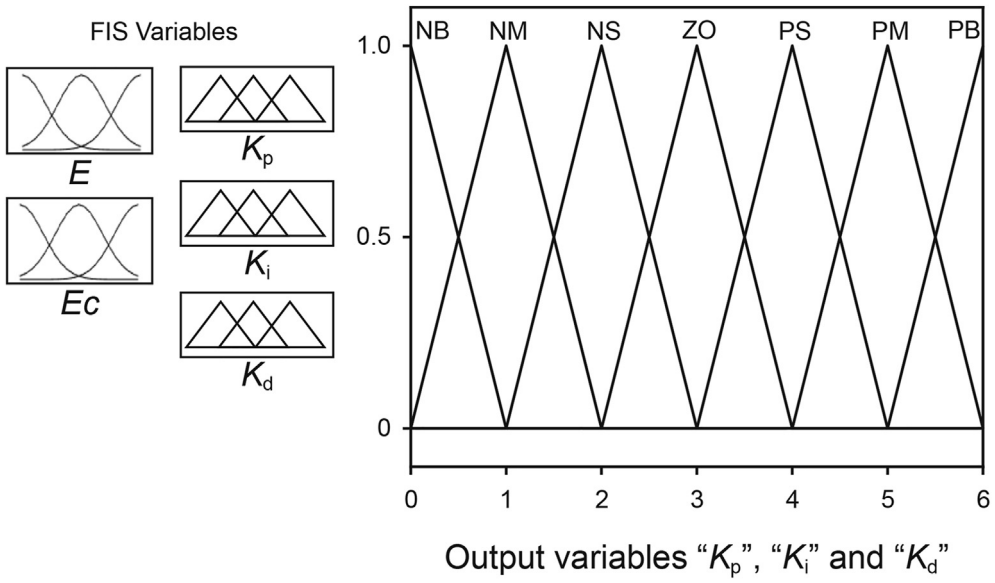

Fig. 15. The membership function of K_p, K_i, K_d

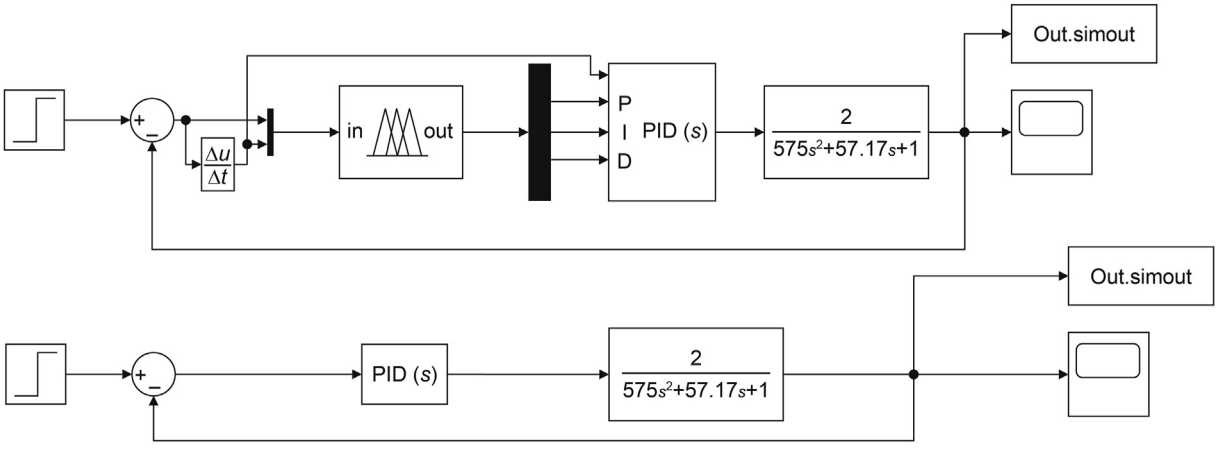

Fig. 16. Fuzzy-PID and PID simulation model in Simulink.

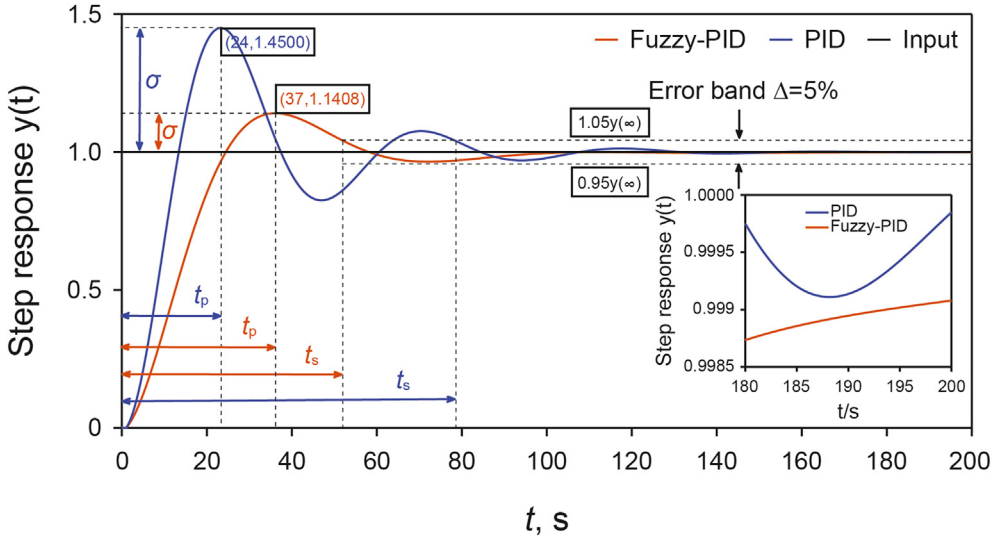

Fig. 17. Step response curve of Fuzzy-PID and PID simulation model.

Table 3
The performance indicators.

Indicators	Overshoot, σ	Peak time, t_p	Adjustment time, t_s
Fuzzy-PID	14%	48.85 s	63.85 s
PID	45%	35.85 s	89.85 s

membership curve are shown in the Fig. 13, Fig. 14 and Fig. 15.

Then design 49 group fuzzy rules according to human operation experience. And establish the simulation model of the heat exchanger outlet temperature control system in Simulink, as shown in Fig. 16. The simulation results are presented in Fig. 17.

It can be observed in Fig. 17 that the performance of Fuzzy-PID control is better than PID control. The overshoot represents the ratio between the maximum deviation of the step response and the steady-state value. The adjustment time represents the time required for the system to reach equilibrium again after being disturbed. The ±5% range of the steady-state value is selected as the error band, which means that the system has reached equilibrium within the error band region. After adopting fuzzy PID control, the overshoot is dramatically reduced, the adjustment time is significantly shortened, and the stability and rapidity of the system are improved. After the adjustment time, the step response of the fuzzy PID control has all been within the error band, that is, the yellow area in the figure. And the PID control system still has not reached the equilibrium state. Amplifying the step response in the 180 s–200 s simulation period, and it can be seen that the volatility of the fuzzy PID control system is obviously smaller than that of the PID control system. The steady-state error of the system is related to the transfer function, and fuzzy PID control and PID control use the same transfer function, so the steady-state error of the two is the same. The calculation method is as follows:

$$e_{ss} = \lim_{s \to 0} s \frac{1}{1 + G(s)} \tag{39}$$

In Eq. (39), e_{ss} represents the steady-state error. By substituting Eq. (38) into Eq. (39), the steady-state error can be calculated as 0.

As the peak time and adjustment time are affected by the pure hysteresis, the actual peak time and adjustment time are 11.85 s later than the simulation results. And the performance indicators of the control system are shown in Table 3.

Therefore, the Fuzzy-PID controller designed in this paper has more superior performance than the traditional PID controller, which provides guidance for the outlet temperature control of the heat exchanger in petrochemical industry.

5. Conclusion

This paper carries out a risk assessment of high-risk heat exchangers in refineries. Through the process simulation calculation, the changes of ammonia and hydrogen chloride partial pressure with temperature are obtained. The crystallization temperature of ammonium salt was produced by Gaussian fitting and chord cut method. Through the comparison of temperature range, it is concluded that the heat exchanger E303 has the risk of corrosion of ammonium salt crystal deposition. Then, the heat exchanger is mathematically modeled to obtain the transfer function of the dynamic characteristics of the heat exchanger as the controlled object of fuzzy control. Through fuzzy PID control, the temperature control of the heat exchanger outlet is achieved. This method has useful application value in oil refining enterprises and can guarantee product quality.

Acknowledgements

This work is supported by the National Natural Science Foundation of China (Grant No. 51876194; U1909216), and General Research Project of Zhejiang Provincial Department of Education (Y201942785).

References

Aras, O., Bayramoglu, M., Hasiloglu, A.S., 2011. Optimization of scaled parameters and setting minimum rule base for a fuzzy controller in a lab-scale pH process. Ind. Eng. Chem. Res. 50 (6), 3335–3344. https://doi.org/10.1021/ie2001023.

Bauer, M., Craig, I.K., 2008. Economic assessment of advanced process control – a survey and framework. J. Process Contr. 18 (1), 2–18. https://doi.org/10.1016/j.jprocont.2007.05.007.

Carvalho, C.B., Carvalho, E.P., Ravagnani, M.A.S.S., 2020. Implementation of a neural network MPC for heat exchanger network temperature control. Braz. J. Chem. Eng. 37 (4), 729–744. https://doi.org/10.1007/s43153-020-00058-2.

Chen, Q., Wang, M., Pan, N., et al., 2009. Optimization principles for convective heat transfer. Energy 34 (9), 1199–1206. https://doi.org/10.1016/j.energy.2009.04.034.

Dulău, M., Karoly, M., Dulău, T., 2018. Fluid temperature control using heat exchanger. Procedia Manufacturing 22, 498–505. https://doi.org/10.1016/j.promfg.2018.03.058.

Faes, W., Lecompte, S., Ahmed, Z.Y., Bael, J.V., Salenbien, R., Verbeken, K., Michel, D.P., 2019. Corrosion and corrosion prevention in heat exchangers. Corrosion Rev. 37 (2), 131–155. https://doi.org/10.1515/corrrev-2018-0054.

Fettaka, S., Thibault, J., Gupta, Y., 2013. Design of shell-and-tube heat exchangers using multiobjective optimization. Int. J. Heat Mass Tran. 60, 343–354. https://doi.org/10.1016/j.ijheatmasstransfer.2012.12.047.

Fuente, M.J., Robles, C., Casado, O., et al., 2006. Fuzzy control of a neutralization process. Eng. Appl. Artif. Intell. 19 (8), 905–914. https://doi.org/10.1016/j.engappai.2006.01.008.

Gang, W.J., Wang, J.B., 2013. Predictive ANN models of ground heat exchanger for the control of hybrid ground source heat pump systems. Appl. Energy 112, 1146–1153. https://doi.org/10.1016/j.apenergy.2012.12.031.

Gao, T.Y., Sammakia, B., Geer, J., 2015. Dynamic response and control analysis of cross flow heat exchangers under variable temperature and flow rate conditions. Int. J. Heat Mass Tran. 81, 542–553. https://doi.org/10.1016/j.ijheatmasstransfer.2014.10.046.

Geng, Z.Q., Zhu, Q.X., 2009. Rough set-based fuzzy rule acquisition and its application for fault diagnosis in petrochemical process. Ind. Eng. Chem. Res. 48, 827–836. https://doi.org/10.1021/ie071171g.

Hojjati, H., Sheikhzadeh, M., Rohani, S., 2007. Control of supersaturation in a semibatch antisolvent crystallization process using a fuzzy logic controller. Ind. Eng. Chem. Res. 46 (4), 1232–1240. https://doi.org/10.1021/ie060967x.

Jia, Y., Chai, T., Wang, H., Su, C., 2020. A signal compensation based cascaded PI control for an industrial heat exchange system. Contr. Eng. Pract. 98, 104372. https://doi.org/10.1016/j.conengprac.2020.104372.

Jin, H.Z., Chen, X.P., Ou, G.F., et al., 2020. Potential failure analysis and prediction of multiphase flow corrosion thinning behavior in the reaction effluent air cooler system. Eng. Fail. Anal. 109, 104274. https://doi.org/10.1016/j.engfailanal.2019.104274.

Jin, H.Z., Chen, X.P., Zheng, Z.J., et al., 2017. Failure analysis of multiphase flow corrosion–erosion with three-way injecting water pipe. Eng. Fail. Anal. 73, 46–56. https://doi.org/10.1016/j.engfailanal.2016.12.005.

Laszczyk, P., 2017. Simplified modeling of liquid-liquid heat exchangers for use in control systems. Appl. Therm. Eng. 119, 140–155. https://doi.org/10.1016/j.applthermaleng.2017.03.033.

Lin, L., Shi, Y., Chen, J.F., et al., 2020. A novel fuzzy PID congestion control model based on cuckoo search in WSNs. Sensors-Basel. 20 (7), 1862. https://doi.org/10.3390/s20071862.

Ou, G.F., Wang, K.X., Zhan, J.L., et al., 2013. Failure analysis of a reactor effluent air cooler. Eng. Fail. Anal. 31, 387–393. https://doi.org/10.1016/j.engfailanal.2013.02.025.

Panahi, H., Eslami, A., Golozar, M.A., Ashrafi Laleh, A., 2020. An investigation on corrosion failure of a shell-and-tube heat exchanger in a natural gas treating plant. Eng. Fail. Anal. 118, 104918. https://doi.org/10.1016/j.engfailanal.2020.104918.

Ramadan, M., Khaled, M., El Hage, H., Harambat, F., Peerhossaini, H., 2016. Effect of air temperature non-uniformity on water–air heat exchanger thermal performance – toward innovative control approach for energy consumption reduction. Appl. Energy 173, 481–493. https://doi.org/10.1016/j.apenergy.2016.04.076.

Rezaei, M., Mahidashti, Z., Eftekhari, S., Abdi, E., 2021. A corrosion failure analysis of heat exchanger tubes operating in petrochemical refinery. Eng. Fail. Anal. 119, 105011. https://doi.org/10.1016/j.engfailanal.2020.105011.

Rhinehart, R., Darby, M.L., Wade, H.L., 2011. Editorial-Choosing advanced control. Isa T 50, 2–10. https://doi.org/10.1016/j.isatra.2010.10.004.

Rizk, T.Y., Al-Nabulsi, K.M., Cho, M.H., 2017. Microbially induced rupture of a heat exchanger shell. Eng. Fail. Anal. 76, 1–9. https://doi.org/10.1016/j.engfailanal.2016.11.004.

Skavdahl, I., Utgikar, V.P., Christensen, R., et al., 2016. Modeling and simulation of control system response to temperature disturbances in a coupled heat exchangers-AHTR system. Nucl. Eng. Des. 300, 161–172. https://doi.org/10.1016/j.nucengdes.2016.01.010.

Vasičkaninová, A., Bakošová, M., čirka, Ľ., et al., 2018. Robust controller design for a laboratory heat exchanger. Appl. Therm. Eng. 128, 1297–1309. https://doi.org/10.1016/j.applthermaleng.2017.09.086.

Wakitani, S., Yamamoto, T., Gopaluni, B., 2019. Design and application of a database-driven PID controller with data-driven updating algorithm. Ind. Eng. Chem. Res. 58 (26SI), 11419–11429. https://doi.org/10.1021/acs.iecr.9b00704.

Wang, L., Jia, Y., Chai, T., Xie, W., 2018. Dual-rate adaptive control for mixed separation thickening process using compensation signal based approach. Ieee T Ind Electron 65 (4), 3621–3632. https://doi.org/10.1109/TIE.2017.2752144.

Wang, S.W., Gao, D.C., Sun, Y.J., et al., 2013. An online adaptive optimal control strategy for complex building chilled water systems involving intermediate heat exchangers. Appl. Therm. Eng. 50, 614–628. https://doi.org/10.1016/j.applthermaleng.2012.06.010.

Xu, X.Q., Bai, Z.Q., Feng, Y.R., et al., 2013. The influence of temperature on the corrosion resistance of 10# carbon steel for refinery heat exchanger tubes. Appl. Surf. Sci. 280, 641–645. https://doi.org/10.1016/j.apsusc.2013.05.038.

Zhang, X.F., Ma, T., Hua, X.C., et al., 2020. Flow accelerated naphthenic acid corrosion during high acid crude oil refining. Eng. Fail. Anal. 104802. https://doi.org/10.1016/j.engfailanal.2020.104802.